Environment and Natural Resources Journal

Volume 24
Issue X
2026

Differential Protein and Morphological Responses of Mosses to Heavy Metal Exposure: Insights from SDS-PAGE Analysis and Microscopic Examination

Supatra Chunchob, Susana Giyasov, Chetsada Phaenark, and Weerachon Sawangproh*

Conservation Biology Program, School of Interdisciplinary Studies, Mahidol University (Kanchanaburi Campus), 199, Moo 9, Lumsum, Saiyok District, Kanchanaburi 71150, Thailand

ARTICLE INFO

Received: 25 Jul 2025
Received in revised: 16 Oct 2025
Accepted: 21 Oct 2025
Published online: 9 Dec 2025
DOI: 10.32526/ennrj/24/20250190

Keywords:
Biomarkers/ Adaptation strategies/ Stress responses/ Housekeeping proteins/ Protein profile

*** Corresponding author:**
E-mail:
weerachon.saw@mahidol.ac.th

ABSTRACT

Heavy-metal pollution poses significant risks to ecosystems and human health. We evaluated acute proteomic and cytological responses of two mosses, *Ectropothecium dealbatum* and *Hyophila involuta*, to cadmium (Cd), lead (Pb), and zinc (Zn). Gametophores were immersed for 72 h to single-metal solutions (10, 20, or 30 mg/L; controls in distilled water), ensuring observed effects reflected single-metal toxicity. Protein profiles were resolved by SDS-PAGE, and light microscopy quantified chloroplasts per lamina cell and the proportion of dead cells. Cd elicited the strongest responses in both species, with intensified high-molecular-weight bands (~90, ~100, ~121 kDa) and pronounced cytological injury; Pb produced qualitatively similar but weaker changes. In contrast, Zn primarily modulated band intensity without generating new bands and caused limited injury at the tested doses. Concordant shifts across methods—reduced chloroplast counts and elevated lamina cell death co-occurring with Cd/Pb-associated bands—support a molecular–physiological linkage of acute metal stress. However, these high-molecular-weight bands (including the ~121 kDa signal) are size-based, putative markers only; independent identification (e.g., LC-MS/MS or immunodetection) and functional validation are still required. Within this 72-h window and concentration range, sensitivity followed Cd > Pb ≫ Zn. The findings nominate candidate proteins for rapid discrimination of damaging (Cd, Pb) versus comparatively tolerated (Zn) exposures and motivate targeted protein identification plus longer, field-calibrated studies to establish biomonitoring thresholds.

HIGHLIGHTS

- SDS-PAGE and microscopy revealed rapid moss responses to heavy metals.
- Cd induced unique 90-121 kDa proteins and severe chloroplast degradation.
- Pb caused weaker but similar proteomic and cytological stress patterns.
- Zn altered band intensity only, showing minimal injury in both mosses
- Cd > Pb ≫ Zn defined toxicity; candidate bands may serve as stress markers.

1. INTRODUCTION

Heavy metal pollution poses a serious threat to environmental and human health. Due to their elemental nature, heavy metals cannot be chemically degraded; thus their detoxification in the environment primarily relies on stabilizing them in place or removing them entirely (Suman et al., 2018). Persistent pollutants such as cadmium (Cd), lead (Pb), and zinc (Zn) originate from both natural processes and various anthropogenic activities, including mining, industrial operations, and agricultural practices (Wuana and Okieimen, 2011). These metals tend to accumulate in soil, water, and organisms, leading to long-term contamination and adverse ecological consequences (Rehman et al., 2013).

The toxicity of heavy metals depends on multiple factors, including their concentration, the plant species involved, and environmental conditions (Cârdei

Citation: Chunchob S, Giyasov S, Phaenark C, Sawangproh W. Differential protein and morphological responses of mosses to heavy metal exposure: Insights from SDS-PAGE analysis and microscopic examination. Environ. Nat. Resour. J. 2026;24(X):xx-xx.

et al., 2021). Among them, cadmium and lead are particularly toxic to plants even at low concentrations (Shukla et al., 2007), as they disrupt essential physiological processes, reduce photosynthetic efficiency, stunt growth, and impair nutrient uptake (Rizvi et al., 2022). On the other hand, zinc toxicity is relatively less common, since zinc is an essential micronutrient required for numerous metabolic functions (Leon-Mediavilla et al., 2018). However, excessive zinc in soil can still be detrimental to plants, producing symptoms similar to those caused by cadmium or lead exposure (Kuziemska et al., 2022).

Bryophytes, including mosses, have increasingly been recognized as effective bioindicators of heavy-metal contamination due to their high surface-area-to-volume ratios (Sun et al., 2009), efficient capacity for metal uptake, and high sensitivity to environmental changes (Stanković et al., 2018), as well as their poikilohydry and widespread distribution across urban, industrial, and remote environments (Tremper et al., 2004; Elliott and Velasquez, 2024). As non-vascular plants that absorb water and nutrients directly from their surroundings, mosses are particularly vulnerable to heavy-metal uptake (Bellini et al., 2021). Understanding how mosses respond to heavy-metal exposure is therefore crucial for accurately assessing contamination levels and formulating effective mitigation strategies (Chaudhuri and Roy, 2024). Mosses serve as sentinel organisms (Świsłowski et al., 2021; Phaenark et al., 2024), reflecting the bioavailability, accumulation, and toxicity of metals in situ. By investigating the molecular mechanisms underlying moss responses, researchers can identify biomarkers of stress and clarify adaptive strategies to cope with metal toxicity (Sun et al., 2011). Acute exposures studies capture the early injury phase—oxidative bursts, rapid chloroplast disruption, and initial cell death—that often precede longer-term acclimation in bryophytes. We therefore profiled short-term (72 h) responses to delineate the immediate injury landscape for Pb, Cd, and Zn as a foundation for subsequent chronic, recovery, and field-relevant studies.

The aim of this study is to examine the physiological and biochemical responses of the moss species *Ectropothecium dealbatum* (Reinw. & Hornsch.) A. Jaeger and *Hyophila involuta* (Hook.) A. Jaeger under exposure to three heavy metals (Cd, Pb, and Zn). Specifically, we analyze protein patterns using sodium dodecyl sulfate-polyacrylamide gel electrophoresis (SDS-PAGE), identify potential biomarkers of heavy-metal exposure through analysis of protein expression patterns (Sardar et al., 2022), and quantify chloroplast numbers and lamina cell death across lamina zones to compare responses under different experimental conditions. Ultimately, this research seeks to inform targeted monitoring and risk assessment for heavy metals—particularly Pb and Cd—while providing mechanistic and phenotypic baselines for future, longer-duration, and field-validated studies.

2. METHODOLOGY

2.1 Plant materials and acclimation

The study involved two moss species: the pleurocarpous moss *E. dealbatum* and the acrocarpous moss *H. involuta*. These species are commonly found year-round in moist areas on the ground at Mahidol University's Kanchanaburi Campus, situated at an altitude of approximately 200 meters above sea level. Species identification was confirmed based on morphological characteristics using a dichotomous key developed by Eddy (1991) and verified by a local bryologist (Mr. Patsakorn Ajintaiyasil, pers. comm.) from Kasetsart University. Moss samples were collected from the university's nursery area adjacent to the campus basketball court (14.129636 N, 99.158747 E) between August and September 2023. During collection, both soil and fresh mosses were carefully gathered using a spatula and placed in multi-purpose zipper bags. We did not characterize soil's metal concentration at the moss collection sites; our study was designed to test acute, controlled exposures under laboratory conditions rather than to correlate moss responses with ambient field contamination. In the laboratory, the mosses were acclimated by transferring them to transparent plastic boxes equipped with ventilation holes and filled with the same soil initially collected with the mosses, which served as a substrate and growth medium. LED bulbs provided a 12-hour lighting source (06:00-18:00 h) on shelves within the chambers, while the air conditioner maintained an ambient temperature of 25±2ºC. Moss samples were watered once daily or as needed to maintain adequate humidity.

2.2 Preparation of metal aqueous solution

Working aqueous solutions (10, 20, and 30 mg/L as metal) of Cd, Pb, and Zn were prepared by diluting certified single-element standards (Merck) with deionized water. For reference, a 1,000 mg/L stock corresponds approximately to 0.009 M

$Cd(NO_3)_2$, 0.005 M $Pb(NO_3)_2$, and 0.015 M $Zn(NO_3)_2$. The pH of all working solutions was adjusted to 5.60±0.02 at 25°C using 6 M NaOH and 6 M HNO_3 as required.

2.3 Heavy metal treatment

Prior to experimentation, fresh gametophores (leafy, stalk-like structures of the gametophyte) with rhizoids removed were collected from the growth chambers, rinsed with tap water, and transferred to clean Petri dishes. Gametophores of *E. dealbatum* or *H. involuta* designated as controls were submerged in 20 mL of distilled water for three days. The remaining gametophores were submerged in 20 mL of heavy metal solutions at concentrations of 10, 20, and 30 mg/L. For each moss species, a total of 27 Petri dishes were prepared (3 metals × 3 concentrations × 3 replicates = 27 Petri dishes). Metal exposure was maintained for three days under LED lighting and controlled air conditioning at 25±2°C (06:00-18:00 hrs). The exposure was limited to three days (72 h) to resolve early, acute responses (protein expression changes, chloroplast loss, cell death) while minimizing potential interference from growth or developmental processes.

2.4 Protein extraction

After 3 days of exposure to metal solutions, 0.3 g of moss gametophores, including leaves and stems, were ground in a pre-chilled pestle and mortar using liquid nitrogen to disrupt cell walls and release proteins. Subsequently, 1,000 µL of lysis buffer containing detergents (1% SDS, 1 M Tris HCl pH 6.8, 2 mM EDTA, 20 mM DTT and 1 × protease inhibitor) for protein solubilization was added, followed by 1,000 µL of distilled water. Once thoroughly mixed, 1,000 µL of the lysate was transferred to a new microcentrifuge tube and centrifuged at 12,000 rpm for 5 min. Later, 600 µL of the lysate was transferred to another new microcentrifuge tube, to which 600 µL of 20% cold TCA was added, thoroughly mixed, and incubated on ice for 60 min for protein precipitation. Once the incubation was finished, the lysate-TCA mixture was centrifuged at 12,000 rpm for 5 min to pellet the precipitated proteins. The clear liquid was decanted, and cold 100% acetone was added to the protein pellet and centrifuged at 12,000 rpm for 5 min to remove contaminants. After decanting the supernatant and a brief air-drying to eliminate residual acetone, the dry pellet was resuspended in 1,000 µL of 80% acetone and centrifuged at 12,000 rpm for 5 min. The clear liquid was decanted once again, and the protein pellet was centrifuged at 12,000 rpm for 2 min. After decanting the clear liquid, the protein pellet was incubated at 55ºC in a water bath for 5 min or until the protein pellet became dry. Finally, the resulting protein pellet was resuspended by adding 70 µL of dissolving buffer (20 mM DTT, 7 M Urea, and 2 M Thiourea) and stored in a fridge at 4ºC for total protein quantification. These techniques were adapted from Barbara et al. (2007).

2.5 Total protein quantification

Total protein content was determined using the Bradford assay with bovine serum albumin (BSA) as the standard, prepared at concentrations ranging from 0 to 1 mg/mL (Bradford, 1976). For the assay, 5 µL of protein samples or BSA standards were pipetted into a 96-well plate, and 250 µL of Bradford reagent was added to each well. The mixtures were thoroughly mixed and incubated at room temperature for 10 minutes to allow dye binding. Absorbance was measured at 595 nm using a microplate spectrophotometer (BMG LabTech, SPECTROstar Nano), with a reagent-only blank as the reference. A standard curve was constructed from the absorbance values of the BSA standards (0.2, 0.4, 0.6, 0.8, 1.0, and 1.2 mg/mL), and protein concentrations of the samples were calculated using the linear regression equation (y=mx). The resulting concentrations (mg/mL) were used to normalize protein input, ensuring equal protein amounts were loaded into each lane for SDS-PAGE analysis.

2.6 Protein separation using SDS-PAGE

Protein separation using SDS-PAGE was conducted using discontinuous buffer systems in Mini PROTEAN® Tetra Cell system from Bio-Rad following a modified procedure (Laemmli, 1970). Initially, 15 µg of extracted proteins were loaded onto a 12% sodium dodecyl sulfate-polyacrylamide gel. The gel cassette was prepared with a 12% separating gel and a 4% stacking gel. The composition of the separating gel included 3.4 mL of distilled water, 2.5 mL of 1.5 M Tris-HCl (pH=8.8), 4 mL of 30% acrylamide, 100 µL of 10% (w/v) SDS, 50 µL of 10% (w/v) APS, and 20 µL of tetramethylene-diamine (TEMED). The stacking gel consisted of 3.1 mL of distilled water, 1.25 mL of 0.5 M Tris-HCl (pH 6.8), 0.65 mL of 30% acrylamide, 100 µL of 10% (w/v) SDS, 50 µL of 10% (w/v) APS, and 10 µL of tetramethylene-diamine (TEMED). The gels were run

in tris-glycine buffer (1 × working solution containing 25 mM Tris-Cl, 250 mM glycine, and 0.1% SDS) at 20 mA/gel for 1.5 hours to induce protein migration based on their molecular size and charge. A pre-stained protein ladder of molecular weight ranging from 10.5 to 175 kDa (Vivantis Technologies Sdn. Bhd.) was used as a standard marker. Following electrophoresis, the gel was stained overnight with Coomassie blue (G-250) protein dye and later de-stained until the background cleared, and protein bands became visible. Finally, the gel was carefully transferred onto a cellophane membrane previously submerged in running buffer. Another cellophane membrane, previously soaked in running buffer, was placed on top of the gel, and the gel was allowed to air dry for visualizing protein banding patterns.

2.7 Microscopic study of lamina cells of mosses

To examine changes in lamina cell structure, gametophore samples were randomly selected from each Petri dish, rinsed with distilled water, and fresh leaves (phyllids) from the middle section of three distinct shoots were chosen using forceps. These leaves were mounted on microscopic slides, covered with coverslips, and observed under a compound light microscope equipped with a digital camera (Nikon DS-Fi3). Following Phaenark et al. (2024), images of the lamina were captured from the basal, median, and apical regions of each leaf and analyzed using NIS-Elements Microscope Imaging Software. Quantitative assessments focused on two key cell characteristics: the number of chloroplasts per lamina cell and the proportion of dead cells, which were compared between heavy-metal-treated moss samples and controls to evaluate stress-induced structural responses.

Counting the chloroplasts in the lamina cells of gametophores in *E. dealbatum* was relatively straightforward because of the leaf lamina's single-cell layer, transparency, and the relatively large chloroplast size. However, counting chloroplasts in the lamina cells of *H. involuta* was challenging due to its papilose cell surface, which hindered clear visualization under the compound microscope. Consequently, only dead cells identified by their distinct brownish color and empty appearance were counted in this species.

2.8 Statistical analyses

The Petri dish was considered the experimental unit (n=3 dishes per species × metal × concentration). Within each metal and lamina zone, concentrations (0, 10, 20, 30 mg/L) were compared using one-way ANOVA when assumptions were met (Shapiro-Wilk on residuals; Levene's test for homogeneity), with Fisher's LSD for post hoc contrasts (α=0.05); when assumptions were violated, we used the Kruskal-Wallis test with Bonferroni-adjusted pairwise comparisons. All analyses were conducted in IBM SPSS Statistics, version 29.

3. RESULTS AND DISCUSSION

3.1 Protein profile based on SDS-PAGE analysis

For years, certain plant species including lower plants such as bryophytes have been suggested as appropriate indicators of pollution (Basile et al., 2013). The use of bryophytes as bioindicators stems from their capacity to accumulate toxic elements, as noted by many authors such as Oishi and Hiura (2017), Stanković et al. (2018), and Printarakul and Meeinkuirt (2022). Bryophytes are effective biomonitors of pollution due to their rapid absorption rate, their ability to absorb substances through their plant surfaces in the absence of roots, and their differential capacity to accumulate a broad spectrum of metals (Rachna and Vashistha, 2017). Previous studies have indicated a considerable sensitivity of certain species to pollution, alongside a notable tolerance in others, as documented by Basile et al. (2005), Esposito et al. (2007), and Esposito et al. (2012). Therefore, the results of our study extend these observations by demonstrating the effects of heavy metal pollution on other bryophyte species as evidenced in protein profile and morphological alteration in lamina cell contents.

The SDS-PAGE analysis of moss protein profiles following exposure to heavy metal exposure provides valuable insights into the adaptive responses of moss species to environmental stressors. The results indicate significant alterations in protein expression in both *E. dealbatum* and *H. involuta* under Cd and Pb treatments, while Zn treatments primarily affected expression levels rather than inducing changes in protein profiles (Figures 1 and 2). Sardar et al. (2022) confirmed that SDS-PAGE is an efficient technique used for enhancing the understanding of plant proteomic modulation under chromium (Cr) stress. Similarly, Gallo et al. (2022) investigated protein profiles in plants from the Brassicaceae family, including both non-metal hyperaccumulators and hyperaccumulators, exposed to nano and ionic forms of Cd and Zn. Their study used 2D SDS-PAGE to

compare protein modulation in response to heavy metals, highlighted differential responses of plant species to metal stress, which aligns with the findings in these moss species.

3.2 Protein expression in *E. dealbatum*

Across all metal treatments (Cd, Pb, Zn), *E. dealbatum* resolved ten SDS–PAGE bands: seven constitutive bands at ~14, 20, 24, 26, 29, 31, and 62 kDa—proteins the cell produces continuously for basic, ongoing functions—and they appeared in every treatment. Three high-molecular-weight bands (90, 100, 121 kDa) varied with metal type and concentration (Figure 1). Under Cd, the 90-, 100-, and 121-kDa bands were upregulated at 10-20 mg/L but declined sharply at 30 mg/L (Figure 1(a)), coinciding with chlorosis of gametophores after three days (Figure 3). This pattern is consistent with the genotoxic and cytotoxic effects of Cd reported for bryophytes (e.g., *Sphagnum palustre*; Sorrentino et al., 2017). With Pb, the same three bands were induced—most clearly at 20-30 mg/L (Figure 1(a))—and plants showed pale laminae (Figure 3), in line with Pb-related disruption of photosynthesis and chlorophyll degradation (Phaenark et al., 2022; Phaenark et al., 2024).

By contrast, Zn did not induce the 90-, 100-, or 121-kDa bands at any concentration (Figure 1(b)). Lamina cell morphology remained unchanged, and no necrosis was observed (Figure 3). Given the stability of the seven constitutive bands across all treatments and the absence of Zn-specific differential bands or visible damage, *E. dealbatum* appears more tolerant to Zn than to Cd or Pb, consistent with Zn's role as an essential plant micronutrient (Stanković et al., 2018).

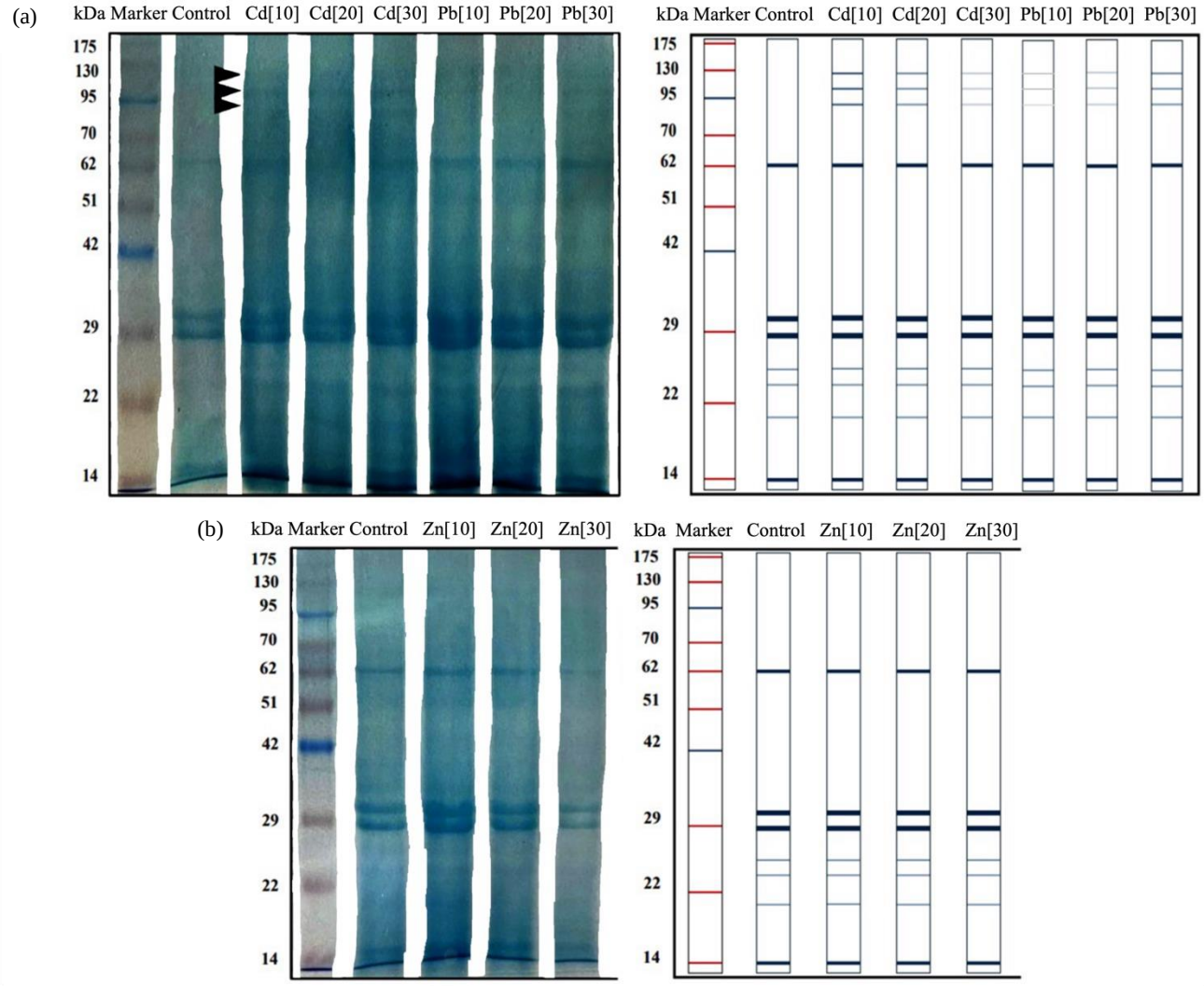

Figure 1. Three proteins, approximately 90, 100, and 121 kilodaltons (kDa) were consistently detected in *E. dealbatum* after the treatment of gametophore (leaves and stems) with Cd and Pb across all concentrations (10, 20, and 30 mg/L) (a). However, these proteins were absent when *E. dealbatum* was subjected to identical concentrations of Zn (b). The left panel displays SDS-PAGE bands, while the right panel illustrates the schematic diagram derived from the protein profile of SDS-PAGE.

3.3 Protein expression in *H. involuta*

We analyzed differential protein expression in *H. involuta* under Cd, Pb, and Zn exposure. Across the control and all metal treatments, *H. involuta* resolved nine SDS-PAGE bands: three high-molecular-weight proteins (~90, 100, and 121 kDa) and six low-molecular-weight proteins (14, 20, 22, 28, 31, and 62 kDa). The high-molecular-weight proteins were clearly up-regulated by Cd at 10-20 mg/L and by Pb at 10-30 mg/L (Figure 2(a)), indicating activation of a conserved heavy-metal stress response (Shafiq et al., 2019). These high-MW bands were not induced by Zn at any concentration (Figure 2(b)).

The six low-molecular-weight proteins were detected in every lane, including the untreated control and all Cd, Pb, and Zn treatments. Under Zn exposure, they exhibited a biphasic pattern—up-regulated at 10-20 mg/L but down-regulated at 30 mg/L relative to the control (Figure 2(b)). This threshold-type response is consistent with Zn's dual role as an essential micronutrient at low levels and a toxicant at high levels that impairs physiology and growth (Akram et al., 2022; Wei et al., 2022). Correspondingly, pronounced lamina alterations and cell death were observed at 30 mg/L Zn (Figure 4), aligning with reports of Zn-induced structural damage in plant tissues (Vijayarengan and Mahalakshmi, 2013).

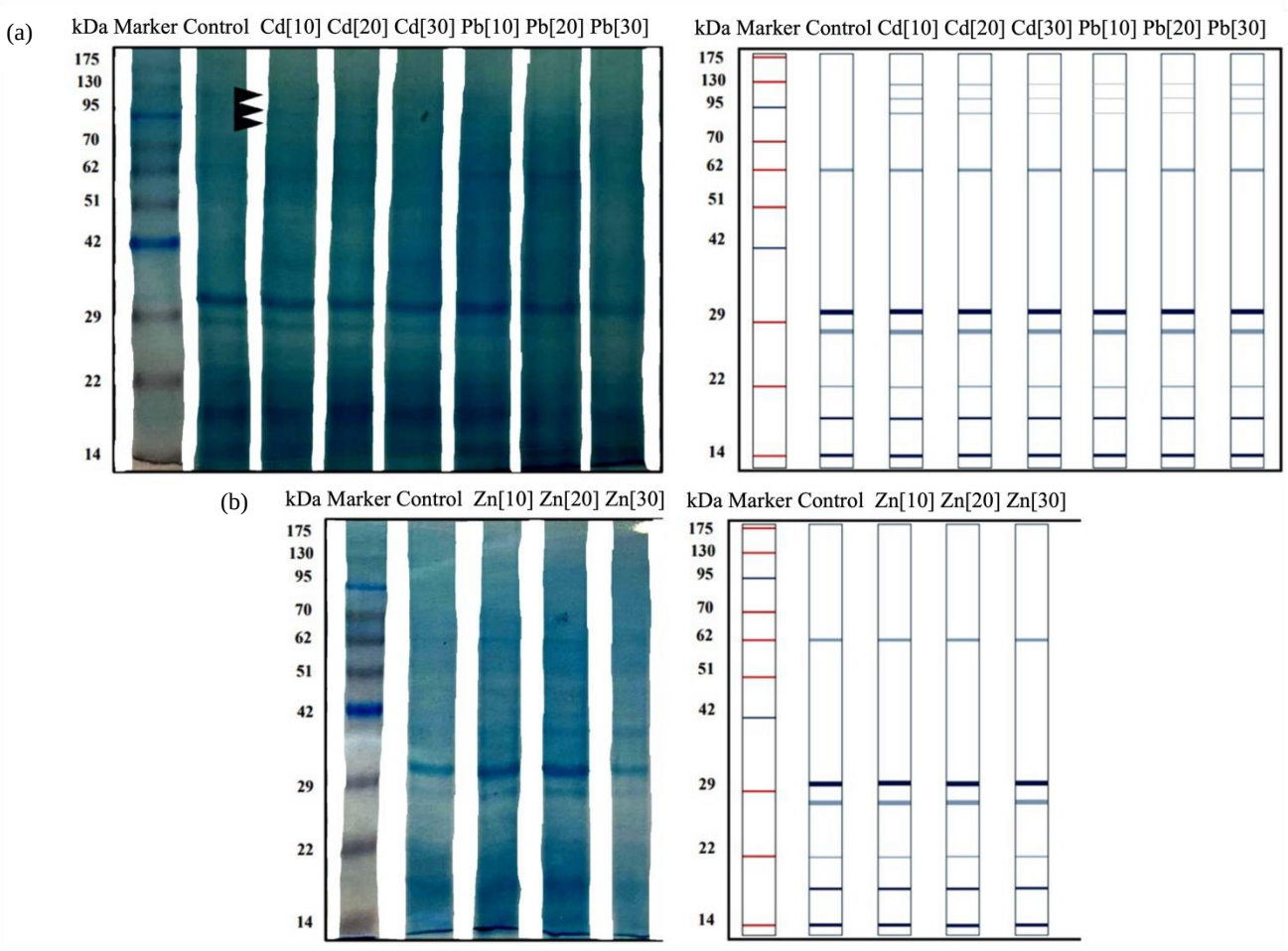

Figure 2. Three proteins, approximately 90, 100, and 121 kilodaltons (kDa) were consistently detected in *H. involuta* after the treatment of gametophore (leaves and stems) with Cd at concentrations of 10, 20, and 30 mg/L, and Pb at 10, 20, and 30 mg/L (a). However, in the lower diagram, these proteins were absent when *H. involuta* was subjected to identical concentrations of Zn (b). The left panel displays SDS-PAGE bands, while the right panel illustrates the schematic diagram derived from the protein profile of SDS-PAGE.

3.4 Stress protein expression in bryophytes under heavy metal exposure

In our study, heavy-metal exposure produced clear protein-expression shifts: bands in the ~90-121 kDa range intensified under Cd and, to a lesser extent, Pb, while Zn elicited little change at the tested doses—suggesting comparatively weaker activation of stress-response pathways. This pattern aligns with established bryophyte responses in which stress proteins commonly appear around ~70, ~90, and ~121 kDa. Heat-shock

proteins (HSP70 at ~70 kDa and HSP90 at ~90 kDa) function as molecular chaperones that stabilize nascent or denatured proteins and limit damage; Pb-exposed *Thuidium qataranse* shows elevated HSPs consistent with tolerance and detoxification (Usman et al., 2022). Because metal stress typically generates reactive oxygen species (ROS), which activate stress-responsive genes including HSPs (Shaheen, 2023), our Cd- and Pb-associated bands are consistent with HSP-mediated defenses. Similar proteomic trends have been reported in higher plants under heavy-metal exposure (Li et al., 2016) and in mosses exposed to Pb and Ni, with pronounced changes in the 70-90 kDa range (Sun et al., 2009).

The ~121 kDa band warrants caution. SDS-PAGE cannot identify proteins or assign them to pathways; migration near ~121 kDa could reflect a large chaperone class (e.g., HSP100-like proteins that cooperate with HSP70/90) or other high-molecular-weight factors associated with oxidative/metal stress (e.g., transport, trafficking, or detoxification proteins). We therefore refrain from assigning protein identities. To progress from patterns to mechanisms, independent techniques based on different principles are required: targeted immunoblotting for candidate chaperones and discovery proteomics (LC-MS/MS peptide mapping, MALDI-TOF profiling) to identify the ~90/~100/~121 kDa species, quantify their regulation across metals and doses, and evaluate post-translational modifications (e.g., phospho-/redox-proteomics) (Shlomi et al., 2006; Parrish et al., 2007).

Once protein identities and their regulatory patterns are validated, integration with network resources (e.g., KEGG, PathBank) and protein-protein interaction data can place these species within chaperone, antioxidant, chelation, and transporter modules, enabling a systems-level view of proteostasis under metal stress (Mlecnik et al., 2005; Nayar and Altman, 2024). At that stage, applied uses—such as developing candidate protein panels to discriminate damaging (Cd, Pb) from comparatively tolerated (Zn) exposures—may be explored, recognizing that any diagnostic thresholds would require calibration against field samples and independent datasets.

In sum, our SDS-PAGE results are consistent with a chaperone-linked stress response under Cd/Pb and a comparatively muted response under Zn; however, definitive protein identities and pathway assignments await targeted immunoblotting and mass-spectrometric confirmation.

3.5 Alteration in chloroplast numbers and lamina cell death

E. dealbatum Chloroplast numbers declined sharply in a dose-dependent manner under Cd across basal, median, and apical zones, with significant reductions beginning at 10 mg/L and the greatest losses at 30 mg/L (e.g., basal: 35±6 → 9±3; median: 29±6 → 8±3; apical: 26±5 → 7±4) (Table 1). Pb caused a milder decline, significant only at 30 mg/L in basal (35±6 → 21±3) and median (29±6 → 18±1) cells, while apical cells were unchanged. Zn produced no significant differences in any zone; means fluctuated but retained control superscripts. In controls (0 mg/L), chloroplast numbers followed basal > median > apical.

Lamina cell mortality increased steeply and dose-dependently under Cd, reaching 92.00% (basal), 88.76% (median), and 70.00% (apical) at 30 mg/L, with the overall mean rising from 0±0 to 83.59±11.88. Pb produced a weaker, zone-specific pattern—apical cells were most sensitive at 20-30 mg/L (56.00-72.88%), median cells rose mainly at 30 mg/L (65.71%), and basal cells changed modestly (~20%). Zn caused negligible mortality at all doses (Table 2). Observations under light microscopy were consistent with these trends (Figure 3).

Table 1. Numbers of chloroplasts in the lamina cells of *E. dealbatum* moss measured across the basal, median, and apical zones of gametophore leaves after exposure to Cd, Pb, and Zn at concentrations of 0, 10, 20, and 30 mg/L.

Concentration of heavy metals	Area of lamina cell		
	Basal cell	Median cell	Apical cell
Cd (mg/L)			
0	35±6^{a}	29±6^{a}	26±5^{a}
10	21±3^{b}	18±4^{b}	15±2^{b}
20	18±3^{b}	15±6^{bc}	11±2^{bc}
30	9±3^{c}	8±3^{c}	7±4^{c}

Table 1. Numbers of chloroplasts in the lamina cells of *E. dealbatum* moss measured across the basal, median, and apical zones of gametophore leaves after exposure to Cd, Pb, and Zn at concentrations of 0, 10, 20, and 30 mg/L (cont.).

Concentration of heavy metals	Area of lamina cell		
	Basal cell	Median cell	Apical cell
Pb (mg/L)			
0	35±6[a]	29±6[a]	26±5[a]
10	31±6[a]	29±3[a]	24±4[a]
20	29±1[a]	27±2[a]	21±3[a]
30	21±3[b]	18±1[b]	17±5[a]
Zn (mg/L)			
0	35±6[a]	29±6[a]	26±5[a]
10	30±7[a]	25±2[a]	28±7[a]
20	34±3[a]	20±1[a]	23±4[a]
30	39±5[a]	25±3[a]	26±5[a]

Remarks: Values represent the mean±standard deviation (SD) (n=3). Different superscript letters within the same column for each heavy metal indicate significant differences (ANOVA followed by Fisher's LSD post-hoc test, equal variance assumed).

Table 2. Percentage of dead lamina cells in *E. dealbatum* moss measured across the basal, median, and apical zones of gametophore leaves after exposure to Cd, Pb, and Zn at concentrations of 0, 10, 20, and 30 mg/L.

Concentration of heavy metals	Area of lamina cell			Overall mean of dead cells in the lamina cells
	Basal cell	Median cell	Apical cell	
Cd (mg/L)				
0	0.00	0.00	0.00	0.00±0.00[a]
10	22.78	8.62	19.00	16.80±7.33[ab]
20	34.29	27.78	22.47	28.18±5.92[ab]
30	92.00	88.76	70.00	83.59±11.88[b]
Pb (mg/L)				
0	0.00	0.00	0.00	0.00±0.00[a]
10	23.91	4.08	16.07	14.69±9.99[ab]
20	8.04	4.17	56.00	22.74±28.87[ab]
30	19.72	65.71	72.88	52.77±28.84[b]
Zn (mg/L)				
0	0.00	0.00	0.00	0.00±0.00[a]
10	0.00	0.00	1.49	0.50±0.86[a]
20	0.00	1.25	4.29	1.85±2.21[a]
30	0.00	0.00	8.24	2.75±4.76[a]

Remarks: Values represent the mean±standard deviation (SD) (n=3). Different superscript letters within each heavy metal treatment indicate significant differences (Kruskal-Wallis test) with Bonferroni-adjusted pairwise comparisons.

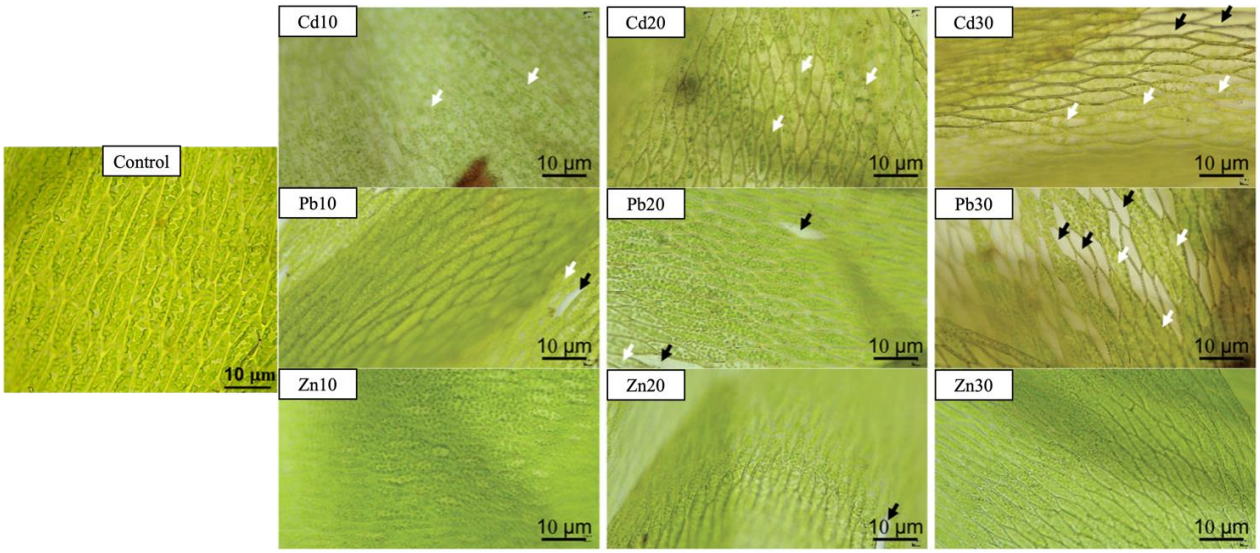

Figure 3. Median cells of the gametophore lamina from *E. dealbatum* were treated with Cd, Pb, and Zn solutions at concentrations of 10, 20, and 30 mg/L. Dead cells are indicated by empty spaces (black arrows) in the figure, while degenerating cells are marked with white arrows. Please note that basal and apical cells of the gametophore lamina were not included in the illustration.

H. involuta Chloroplast numbers could not be reliably quantified because papillose leaf cells obscured chloroplast visibility (Figure 4). Nevertheless, Cd elicited pronounced basal-zone vulnerability, with 100% cell death at 10-30 mg/L, whereas median and apical zones increased only slightly (≤17.05% and ≤3.33%). Pb and Zn had minimal effects across zones (overall means ≤10.21% and ≤2.51%, respectively), with no significant deviations from control (Table 3).

Table 3. Percentage of dead lamina cells in *H. involuta* moss measured across the basal, median, and apical zones of gametophore leaves after exposure to Cd, Pb, and Zn at concentrations of 0, 10, 20, and 30 mg/L.

Concentration of heavy metals	Area of lamina cell			Mean of dead cells in the lamina cells
	Basal cell	Median cell	Apical cell	
Cd (mg/L)				
0	0.00	0.00	0.00	0.00±0.00[a]
10	100.00	1.24	0.48	33.91±57.24[a]
20	100.00	3.13	2.34	35.16±56.16[a]
30	100.00	17.05	3.33	40.13±52.30[a]
Pb (mg/L)				
0	0.00	0.00	0.00	0.00±0.00[a]
10	3.79	0.19	3.57	2.52±2.02[a]
20	4.24	7.02	2.42	4.56±2.32[a]
30	20.42	6.97	3.25	10.21±9.03[a]
Zn (mg/L)				
0	0.00	0.00	0.00	0.00±0.00[a]
10	4.37	0.00	0.56	1.64±2.38[a]
20	0.00	0.00	1.11	0.37±0.64[a]
30	1.74	3.79	2.00	2.51±1.12[a]

Remarks: Values represent the mean±standard deviation (SD) (n=3). Different superscript letters within each heavy metal treatment indicate significant differences (Kruskal-Wallis test) with Bonferroni-adjusted pairwise comparisons.

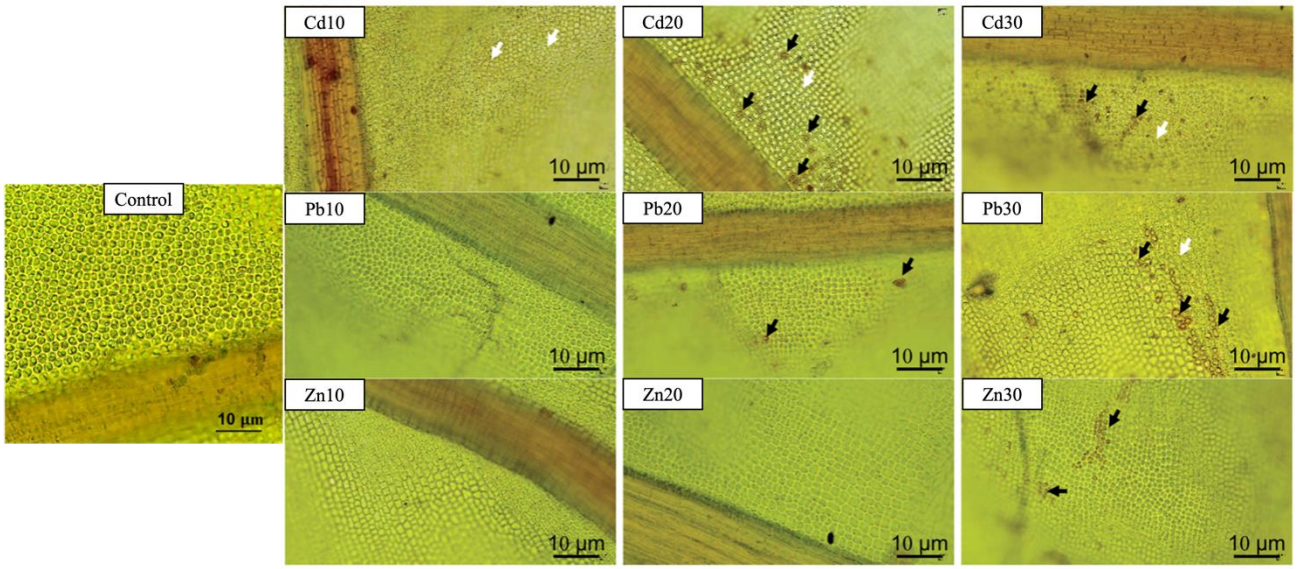

Figure 4. Median cells of gametophore lamina from *H. involuta* were treated with Cd, Pb, and Zn solutions at concentrations of 10, 20, and 30 mg/L. Dead cells are indicated by empty spaces (black arrows) in the figure, while degenerating cells are marked with white arrows. Please note that basal and apical cells of the gametophore lamina were not included in the illustration.

Overall, our findings show that Cd imposes the strongest stress on both mosses: in *E. dealbatum* through concordant losses in chloroplast numbers and large increases in lamina cell death, and in *H. involuta* through extreme basal-zone mortality. Such outcomes align with Cd's well-documented genotoxic and cytotoxic effects that compromise photosynthetic capacity and cellular integrity in other bryophytes (Sorrentino et al., 2017). Pb effects were weaker and zone-dependent, consistent with reports of

Pb-induced disruption of photosynthesis and chlorophyll stability that is often less acute than Cd (Phaenark et al., 2022; Phaenark et al., 2024). The observed species- and zone-specific patterns likely reflect anatomical and physiological differences; in *H. involuta*, basal-zone susceptibility to Cd may relate to local variation in uptake or sequestration pathways (Phaenark et al., 2022; Phaenark et al., 2024).

Zn was largely innocuous at the concentrations tested, producing no significant mortality and no notable changes in chloroplast counts. A slight, non-significant tendency toward higher chloroplast numbers in *E. dealbatum* under Zn is consistent with Zn's essential role and reports of Zn-stimulated pigment accumulation in some plants (Dang et al., 2024), while the broader literature cautions that excess Zn can still impair physiology depending on dose and context (Vijayarengan and Mahalakshmi, 2013; Akram et al., 2022; Wei et al., 2022). Because soils were not analyzed at collection sites, we cannot relate baseline field metal burdens to the laboratory responses. This is unlikely to confound our acute outcomes—the exposure solutions dominated metal availability over 72 h—but it does limit inference about how pre-exposure history might shape proteomic baselines. The absence of site-soil chemistry prevents us from assessing prior metal exposure or edaphic modifiers (pH, organic matter, texture) that can influence bioavailability. Future work should pair moss sampling with standardized soil digests (e.g., EPA 3051A/ISO 11466) and porewater extractions to calibrate biomarker bands against environmentally realistic concentrations. Together with microscopy (Figures 3 and 4), these results highlight Cd as the dominant driver of physiological damage, Pb as a moderate, zone-specific stressor, and Zn as largely non-damaging in this study, underscoring the value of mosses as bioindicators of heavy-metal pollution.

Consistent with the physiological outcomes, both moss species showed co-induction of ~90, ~100, and ~121 kDa bands under Cd (and to a lesser extent Pb), whereas Zn did not alter the overall banding pattern but only modulated band intensity. Under acute (72 h) exposure across 10-30 mg/L, this dose- and time-spanning concordance between high-molecular-weight band induction and chloroplast loss/lamina cell death supports these bands as candidate biomarkers of metal-induced damage. In contrast, the stability of constitutive bands (≈14-62 kDa) provides an internal reference for tolerance. Mechanistically, the ~90-121 kDa window plausibly includes stress-chaperone proteins (e.g., HSP90/ HSP100) involved in proteostasis; their lack of induction under Zn aligns with the negligible cytological injury observed at the tested doses.

4. CONCLUSION

This study compared the short-term (72 h) responses of two common mosses, *E. dealbatum* and *H. involuta*, to Cd, Pb, and Zn under controlled laboratory conditions. Both species were more tolerant to Zn than to Pb or Cd, but the degree and pattern of sensitivity differed between species. In *E. dealbatum*, Cd caused a pronounced, dose-dependent loss of chloroplasts across lamina zones together with large increases in cell death, whereas Pb produced weaker, zone-specific effects. In *H. involuta*, chloroplast numbers could not be reliably quantified due to papillose cells, yet Cd still triggered severe basal-zone mortality, with only modest changes under Pb and minimal effects under Zn. Overall, the toxicity gradient followed Cd > Pb ≫ Zn, with species-specific manifestations (photosynthetic impairment and widespread mortality in *E. dealbatum* versus localized, basal-zone vulnerability in *H. involuta*). Proteomically, Cd and, to a lesser extent, Pb elicited high-molecular-weight SDS-PAGE bands (~90, ~100, ~121 kDa) that coincided with chloroplast loss and/or lamina cell death, whereas Zn primarily altered band intensity without changing overall patterns. These findings indicate an acute molecular–physiological association under Cd/Pb exposure rather than demonstrating long-term adaptation.

The present results suggest that these two mosses may have potential for targeted assessments of Cd and Pb under controlled conditions; however, we do not conclude that they are established bioindicators of metal pollution. Confirmation will require independent validation of the putative biomarker bands (e.g., immunoblotting, LC-MS/MS), longer and chronic exposures, environmentally realistic mixtures, and field calibration against measured metal levels. Because soils were not analyzed at collection sites, we cannot relate baseline field metal burdens to the observed laboratory responses; this limits inference about how prior exposure histories could shape proteomic baselines. Accordingly, future work should (i) expand to other metals/metalloids and mixtures, (ii) incorporate time-course dose-response designs over

longer durations, (iii) identify and verify differentially expressed proteins, and (iv) pair moss sampling with standardized soil digests and porewater extractions to derive field-relevant thresholds before any operational biomonitoring is proposed.

ACKNOWLEDGEMENTS

The authors would like to acknowledge the Science Laboratory for Education (SLE) at Mahidol University (Kanchanaburi Campus) for providing laboratory facilities.

AUTHOR CONTRIBUTIONS

Supatra Chunchob: Conceptualization, Methodology, Software, Validation, Formal analysis, Investigation, Resources, Data curation, Writing-original draft preparation, Writing-review and editing, Visualization, Supervision, Project administration. Susana Giyasov: Validation, Formal analysis, Investigation, Resources, Data curation. Chetsada Phaenark: Validation, Formal analysis, Investigation, Resources, Data curation, Writing-original draft preparation, Writing-review and editing. Weerachon Sawangproh: Conceptualization, Methodology, Validation, Investigation, Writing-original draft preparation, Writing-review and editing, Visualization, Supervision. All authors have read and agreed to the published version of the manuscript.

DECLARATION OF CONFLICT OF INTEREST

The authors declare that they have no known competing financial interests or personal relationships that could have appeared to influence the work reported in this paper.

REFERENCES

Akram MW, Sajid M, Ahmad A, Waqar M, Kusar S, Iqbal A, et al. Effect of foliar spray of ascorbic acid on nodulation, gas exchange attributes and mineral ion contents of *Pisum sativum* under zinc stress. Plant Protection 2022;6(2):101-11.

Barbara C, Braglia R, Basile A, Cobianchi RC, Forni C. Proteomics and bryophytes: A comparison between different methods of protein extraction to study protein synthesis in the aquatic moss *Leptodictyum riparium* (Hedw.). Caryologia 2007;60(1-2):102-5.

Basile A, di Nuzzo RA, Capasso C, Sorbo S, Capasso A, Carginale V. Effect of cadmium on gene expression in the liverwort *Lunularia cruciata*. Gene 2005;356:153-9.

Basile A, Sorbo S, Conte B, Cardi M, Esposito S. Ultrastructural changes and Heat Shock Proteins 70 induced by atmospheric pollution are similar to the effects observed under in vitro heavy metals stress in *Conocephalum conicum* (Marchantiales-Bryophyta). Environmental Pollution 2013; 182:209-16.

Bellini E, Betti C, Sanità di Toppi L. Responses to cadmium in early-diverging Streptophytes (Charophytes and Bryophytes): Current views and potential applications. Plants 2021; 10(4):Article No. 770.

Bradford MM. A rapid and sensitive method for the quantitation of microgram quantities of protein using the principle of protein dye binding. Analytical Biochemistry 1976;72(1-2):248-54.

Cârdei P, Tudora C, Vlăduț V, Pruteanu MA, Găgeanu I, Cujbescu D, et al. Mathematical model to simulate the transfer of heavy metals from soil to plant. Sustainability 2021;13(11):Article No. 6157.

Chaudhuri S, Roy M. Global ambient air quality monitoring: Can mosses help? A systematic meta-analysis of literature about passive moss biomonitoring. Environment, Development and Sustainability 2024;26:5735-73.

Dang K, Mu J, Tian H, Gao D, Zhou H, Guo L, et al. Zinc regulation of chlorophyll fluorescence and carbohydrate metabolism in saline-sodic stressed rice seedlings. BMC Plant Biology 2024;24(1):Article No. 464.

Eddy A. A Handbook of Malesian Mosses. Vol. 2 Leucobryaceae to Buxbaumiacea. London, UK: Natural History Museum Publications; 1991.

Elliott DD, Velasquez PM. Non-vascular plants [Internet]. 2024 [cited 2024 July 23]. Available from: https://bio.libretexts.org/Bookshelves/Botany/Botany_in_Hawaii_(Daniela_Dutra_Elliott_and_Paula_Mejia_Velasquez)/06%3A_Plant_evolution_and_non-vascular_plants/6.03%3A_Non-vascular_plants.

Esposito S, Cobianchi RC, Sorbo S, Conte B, Basile B. Ultrastructural alterations and HSP70 induction in *Elodea canadensis* Michx. exposed to heavy metals. Caryologia 2007;60(1-2):115-20.

Esposito S, Sorbo S, Conte B, Basile A. Effects of heavy metals on ultra- structure and HSP70s induction in the aquatic moss *Leptodictyum riparium* Hedw. International Journal of Phytoremediation 2012;14(4):1-13.

Gallo V, Serianni VM, Imperiale D, Zappettini A, Villani M, Marmiroli M, et al. Protein analysis of *A. halleri* and *N. caerulescens* hyperaccumulators when exposed to nano and ionic forms of Cd and Zn. Nanomaterials 2022;12(23):Article No. 4236.

Kuziemska B, Klej P, Wysokiński A, Jaremko D, Pakuła K. Yielding and bioaccumulation of zinc by cocksfoot under conditions of different doses of this metal and organic fertilization. Agronomy 2022;12(3):Article No. 686.

Laemmli UK. Cleavage of structural proteins during the assembly of the head of bacteriophage T4. Nature 1970;227:680-5.

Leon-Mediavilla J, Senovilla M, Montiel J, Gil-Diez P, Saez A, Kryvoruchko IS, et al. MtMTP2-facilitated zinc transport into intracellular compartments is essential for nodule development in *Medicago truncatula*. Frontiers in Plant Science 2018;9:Article No. 990.

Li GK, Gao J, Peng H, Shen Y, Ding H, Zhang ZM, et al. Proteomic changes in maize as a response to heavy metal (lead) stress revealed by iTRAQ quantitative proteomics. Genetics and Molecular Research 2016;15(1):1-14.

Mlecnik B, Scheideler M, Hackl H, Hartler J, Sánchez-Cabo F, Trajanoski Z. PathwayExplorer: web service for visualizing high-throughput expression data on biological pathways. Nucleic Acids Research 2005;33:633-7.

Nayar G, Altman R. Heterogeneous network approaches to protein pathway prediction. Compuational and Structural Biotechnology Journal 2024;23:2727-39.

Oishi Y, Hiura T. Bryophytes as bioindicators of the atmospheric environment in urban-forest landscapes. Landscape and Urban Planning 2017;167:348-55.

Parrish J, Yu J, Liu G, Hines J, Chan J, Mangiola B, et al. A proteome-wide protein interaction map for *Campylobacter jejuni*. Genome Biology 2007;8:Article No. R130.

Phaenark C, Niamsuthi A, Paejaroen P, Chunchob S, Cronberg N, Sawangproh W. Comparative toxicity of heavy metals Cd, Zn, and Pb to three acrocarpous moss species using chlorophyll contents. Trends in Sciences 2022;20(2):Article No. 4287.

Phaenark C, Seechanhoi P, Sawangproh W. Metal toxicity in *Bryum coronatum* Schwaegrichen: Impact on chlorophyll content, lamina cell structure, and metal accumulation. International Journal of Phytoremediation 2024;26(8): 1336-47.

Printarakul N, Meeinkuirt W. The bryophyte community as bioindicator of heavy metals in a waterfall outflow. Scientific Reports 2022;12(1):Article No. 6942.

Rachna P, Vashistha BD. Effects of heavy metals on protonemal growth and bud formation in the moss *Hydrogonium arcuatum*. Agricultural Science Digest 2017;37(2):117-21.

Rehman K, Ashraf S, Rashid U, Ibrahim M, Hina S, Iftikhar T, et al. Comparison of proximate and heavy metal contents of vegetables grown with fresh and wastewater. Pakistan Journal of Botany 2013;45(2):391-400.

Rizvi A, Ahmed B, Khan MS, Rajput VD, Umar S, Minkina T, et al. Maize associated bacterial microbiome linked mitigation of heavy metal stress: A multidimensional detoxification approach. Environmental and Experimental Botany 2022; 200:Article No. 104911.

Sardar R, Zulfiqar A, Ahmed S, Shah AA, Iqbal RK, Hussain S, et al. Proteomic changes in various plant tissues associated with chromium stress in sunflower. Saudi Journal of Biological Sciences 2022;29(4):2604-12.

Shafiq S, Zeb Q, Ali A, Sajjad Y, Nazir R, Widemann E, et al. Lead, cadmium and znc phytotoxicity alter DNA methylation levels to confer heavy metal tolerance in wheat. International Journal of Molecular Sciences 2019;20(19):Article No. 4676.

Shaheen S, Majeed Z, Mahmood Q. The assessment of metal resistance through the expression of hsp-70 and ho-1 proteins in giant reed. International Journal of Plant Biology 2023;14(3):687-700.

Shlomi T, Segal D, Ruppin E, Sharan R. QPath: A method for querying pathways in a protein-protein interaction network. BMC Bioinformatics 2006;7:Article No. 199.

Shukla SR, Rao RV, Sharma SK, Kumar P, Sudheendra R, Shashikala S. Physical and mechanical properties of plantation-grown *Acacia auriculiformis* of three different ages. Australian Forestry 2007;70(2):86-92.

Sorrentino MC, Capozzi F, Giordano S, Spagnuolo V. Genotoxic effect of Pb and Cd on in vitro cultures of *Sphagnum palustre*: An evaluation by ISSR markers. Chemosphere 2017;181: 208-15.

Stanković J, Sabovljević A, Sabovljević MS. Bryophytes and heavy metals: A review. Acta Botanica Croatica 2018; 77(2):109-18.

Suman J, Uhlik O, Viktorova J, Macek T. Phytoextraction of heavy metals: A promising tool for clean-up of polluted environment? Frontiers in Plant Science 2018;9:Article No. 1476.

Sun S-Q, He M, Cao T, Zhang Y-C, Han W. Response mechanisms of antioxidants in Bryophyte (*Hypnum plumaeforme*) under the stress of single or combined Pb and/or Ni. Environmental Monitoring and Assessment 2009;149(1-4):291-302.

Sun SQ, He M, Wang GX, Cao T. Heavy metal-induced physiological alterations and oxidative stress in the moss *Brachythecium piligerum* chad. Environmental Toxicology 2011;26(5):453-8.

Świsłowski P, Nowak A, Rajfur M. The influence of environmental conditions on the lifespan of mosses under long-term active biomonitoring. Atmospheric Pollution Research 2021;12(10):Article No. 101203.

Tremper AH, Agneta M, Burton S, Higgs DEB. Field and laboratory exposures of two moss species to low level metal pollution. Journal of Atmospheric Chemistry 2004;49:111-20.

Usman K, Souchelnytskyi S, Zouari N, Abu-Dieyeh MH. Proteomic analysis of *T. qataranse* exposed to lead (Pb) stress reveal new proteins with potential roles in Pb tolerance and detoxification mechanism. Frontiers in Plant Science 2022;13:Article No. 1009756.

Vijayarengan P, Mahalakshmi G. Zinc toxicity in tomato plants. World Applied Sciences Journal 2013;24(5):649-53.

Wei C, Jiao Q, Agathokleous E, Liu H, Li G, Zhang J, et al. Hormetic effects of zinc on growth and antioxidant defense system of wheat plants. Science of the Total Environment 2022;807(Part 2):Article No. 150992.

Wuana RA, Okieimen FE. Heavy metals in contaminated soils: A review of sources, chemistry, risks and best available strategies for remediation. International Scholarly Research Notices 2011;2011(1):Article No. 402647.